Calibration of Microwave Reference Blackbodies and Targets for Use in Satellite Observations: An Analysis of Errors in Theoretical Outlooks and Testing Procedures

Pierre-Marie Robitaille

Department of Radiology, The Ohio State University, 395 W. 12th Ave, Suite 302, Columbus, Ohio 43210, USA
E-mail: robitaille.1@osu.edu

Microwave reference blackbodies and targets play a key role in astrophysical and geophysical studies. The emissivity of these devices is usually inferred from return-loss experiments which may introduce at least 10 separate types of calibration errors. The origin of these inaccuracies depends on test conditions and on the nature of each target. The most overlooked errors are related to the geometry adapted in constructing reference loads and to the effects of conduction or convection. Target shape and design can create an imbalance in the probabilities of absorption and emission. This leads to loss of radiative equilibrium, despite the presence of a thermodynamic steady state. Heat losses or gains, through conduction and convection, compensate for this unexpected physical condition. The improper calibration of blackbodies and targets has implications, not only in global climate monitoring, but also relative to evaluating the microwave background.

1 Introduction

Blackbodies [1–4] can be difficult to construct and analyze. For example, by unknowingly pumping normal radiation [2, 3] into cavities using their detectors, scientists can easily make the interior of enclosures appear black [4]. They thereby create the illusion that all cavities emit normal radiation [1–3]. Relative to microwave reference targets, the situation is further complicated by the realization that these devices are pseudo-cavities and become subject to geometrical considerations. These problems are important as microwave targets are present on numerous satellites monitoring the microwave background [5–7] and global climate (e.g. [8]).

Calibration targets for microwave frequencies [9–15] are typically made from carbon or iron containing foams and epoxy resins, such as Eccosorb foams and Eccosorb CR-110 and 117 [Emerson and Cuming, Randolph, MA]. Recently, an aqueous blackbody has been proposed for calibration purposes [16]. Such a device takes advantage of the powerful microwave absorbance of water. As for Eccosorb surfaces used in the microwave [5,7], unlike graphite and carbon black paints in the infrared [3, 17–20], they manifest significantly increased absorbance as a function of thickness. Therefore, it is impossible to obtain a blackbody emission from a thin layer of Eccosorb, irrespective of claims to the contrary. For example, a 1 cm layer of Eccosorb CR-110 has an absorbance of only ∼6 dB at 18 GHz [21]. Despite this reality, space restrictions aboard spacecraft often limit the volume available for satellite reference targets [7]. Further complicating the situation, these materials permit transmission at microwave frequencies and are not opaque. Consequently, the correct treatment of their properties involves the consideration of transmission. Unfortunately, since reference targets are often backed by highly reflective metal casings [10–15], it becomes easy to ignore the effects of transmission in the absorber. This can lead to a serious overestimation of calibrator emissions, as will be demonstrated.

2 The testing of reference targets

Almost without exception, the testing of microwave reference targets involves their placement within an anechoic chamber (e.g. [10–15]). Here, they are subjected to incident microwave radiation emitted from a test horn, typically driven at the frequency of interest by a network analyzer. This is achieved while making the assumption that the target, with its absorbing material and metal casing (e.g. [10–15]), can be treated as a single opaque unit. By measuring the return-loss produced in this configuration, the emissivity of the target can be inferred, but not without risk of error.

Return loss measurements are based on the validity of Stewart's formulation, which advances the equivalence of emission and absorption under conditions of thermal equilibrium [22, 23]. This statement is commonly viewed by the scientific community as Kirchhoff's law [1]. However, Kirchhoff's law differs from Stewart's formulation by advocating that all radiation within cavities must be black. Such a concept is demonstrably false [4, 17, 23]. As a result, the law of equivalence between emissivity and absorptivity, must be attributed uniquely to Stewart [22, 23].

The emissivity of a target is usually estimated through the relationship $\varepsilon_t = 1 - \sigma_{tn}$, where ε_t and σ_{tn} represent target emissivity and normal reflectivity, respectively (i.e. [10–15]. This treatment assumes that only normal reflection takes place and also constitutes an implicit formulation of Stewart's law [23]. Nonetheless, in this discussion, we will consider the

measurement of absorption, rather than emission, and write $\kappa_t = 1 - \sigma_{tn}$, where κ_t represents the absorptivity of the target. In the end, it is demonstrated that the measurement of absorptivity from return loss measurements in no way implies that the emissivity of the target has been properly evaluated.

2.1 Type-1, -2, -3 and -4 errors

The first error in the determination of emissivity using return loss measurements, involves leakage of incident radiation from the horn, directly into the anechoic chamber, without ever striking the target. This will be referred to as a Type-1 error (see Figure 1A) and symbolized as Γ_{bp}, as it depends on the beam pattern of the horn. Type-2 errors can occur when incident radiation is diffracted around the edges of the horn on transmission, as shown in Figure 1A. Type-2 errors will be symbolized as Γ_{dh} as they represent diffraction on the horn. These errors are also associated with the beam pattern. Since corrugated edging can be placed on a horn to minimize the effects of diffraction, it is treated as a separate error. Type-3 errors are similar in nature to Type-2 errors, but involve the diffraction of incoming radiation on the edges of the target, Γ_{dt}. This term also includes radiation which is scattered by the target. Finally, a Type-4 error results from the neglect of diffuse reflection off the target surface, σ_{td}.

Each of these error types result in radiation being lost to the walls of the anechoic chamber. Such radiation will not be available to the horn and will subsequently contribute to lowering the measured return radiation. In order to overcome this problem, it is important to numerically evaluate the beam pattern of the horn, thereby inferring the percentage of incident radiation that does, in fact, strike the target. It is also possible to place pick-up horns in the anechoic chamber and evaluate the beam patterns directly, in the absence of a target. Thus, whether through calculations or direct measurement, the magnitude of these errors can be understood and are usually properly addressed. Nonetheless, and for the sake of completeness, it is clear that the absorptivity of the target is actually given by:

$$\kappa_t = 1 - \sigma_{tn} - \sigma_{td} - \Gamma_{bp} - \Gamma_{dh} - \Gamma_{dt}. \qquad (1)$$

When viewing the target as a single unit, Type-1, -2, -3, and -4 errors can lead to the inaccurate assessment of target emissivity from return-loss experiments. Yet, it is the effect of using a transmissive absorber, in the presence of a metal casing or support, which can lead to the greatest errors in evaluating emissivity.

2.2 Type-5 and -6 errors

The emissivity of microwave targets is exclusively dominated by an absorbing material, like Eccosorb, which is also transmissive [9, 21]. Accordingly, it is unwise to treat these devices as single units. Instead, clearer insight into the problem can be gained if one views the target as made from its two
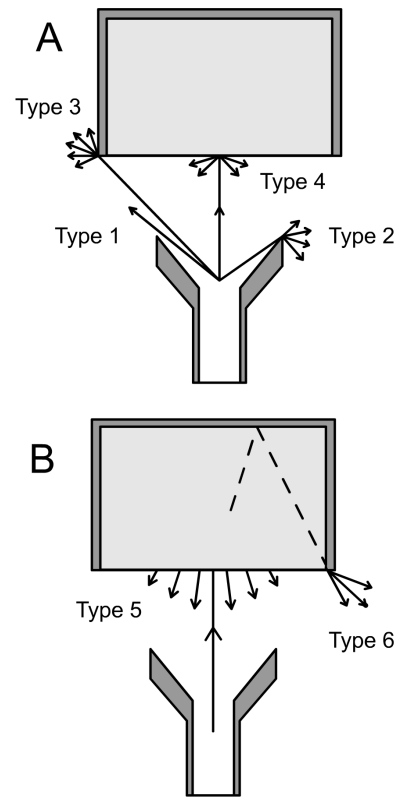

Fig. 1: Schematic representation of error types when assessing effective emissivity using return-loss measurements.

components: the absorbent material and the perfectly reflective metallic backing. In this scenario, the absorbent material can be considered as possessing absorptivity, κ_a, and emissivity, ε_a, equal to one another ($\kappa_a = \varepsilon_a$), along with normal reflectivity, σ_{an}, diffuse reflectivity, σ_{ad}, and transmissivity, τ_a. The metallic casing, c, often constructed from aluminum, is viewed as having perfect reflectivity ($\sigma_c = 1$).

Under such conditions, the difficulties in ascertaining the emissivity of the target become evident, since for any non-opaque substance, $\varepsilon = 1 - \sigma - \tau$, rather than $\varepsilon = 1 - \sigma$. Because the absorber has transmittance, it can permit microwave energy to pass through its body and strike the metallic backing at virtually any angle. While an object transmits incident radiation, it is not required to preserve either phase or angle of incidence. As such, when the transmitted component strikes the casing, it can do so in a manner whereby the microwave energy, following reflection, re-enters the absorber only to be absorbed, transmitted towards the horn, scattered into space, or diffracted by the edge of the casing. This would lead to a good return-loss measurement on the network analyzer; but it would be improper to assume that $\varepsilon = 1 - \sigma$. Therefore, it becomes nearly impossible to measure emissivity, as will be demonstrated.

In reality, by treating the target as an opaque unit made up of two components (i.e. the absorber and the reflective

casing), it is apparent that its absortivity is now given by:

$$\kappa_t = 1 - \sigma_{an} - \sigma_{ad} - \Gamma_{bp} - \Gamma_{dh} - \Gamma_{dc} -$$
$$- \kappa_a \tau_a \sigma_c - \tau_a \tau_a \sigma_c - s_a \tau_a \sigma_c - d_a \tau_a \sigma_c , \quad (2)$$

where the normal and diffuse reflection of the absorber are now being considered (σ_{an} and σ_{ad}), along with the diffraction of incident radiation on the casing, Γ_{dc} (previously viewed as Γ_{dt}), and four new terms arise, whose coefficients sum to 1 (i.e. $\kappa_a + \tau_a + s_a + d_a = 1$). The seventh term, $\kappa_a \tau_a \sigma_c$, corresponds to that fraction of transmitted power which is reflected by the casing, σ_c, and absorbed, κ_a, upon reentry into the absorber. The eighth term, $\tau_a \tau_a \sigma_c$, represents that fraction of the transmitted power which is reflected by the casing and is subsequently re-transmitted, τ_a, towards the horn. The seventh term, like the eighth term, has been innocently considered when treating the target as an opaque unit in section 2.1. These terms introduce no errors in the return-loss measurement itself. For instance, it is evident that, with rearrangement, Eq. (2) becomes:

$$\kappa_{t_{\text{eff}}} = (\kappa_t + \kappa_a \tau_a \sigma_c) = 1 - (\sigma_{an} + \tau_a \tau_a \sigma_c) - \sigma_{ad} -$$
$$- \Gamma_{bp} - \Gamma_{dh} - \Gamma_{dc} - s_a \tau_a \sigma_c - d_a \tau_a \sigma_c . \quad (3)$$

In this expression, the seventh term in Eq. (2), $\kappa_a \tau_a \sigma_c$, is moved to the left as it makes a positive contribution to the effective absorptivity of the target, where on measurement, κ_t is indistinguishable from $\kappa_a \tau_a \sigma_c$. Unfortunately, we must now consider the effective absorptivity, $\kappa_{t_{\text{eff}}}$, from the target. In fact, the seventh term, $\kappa_a \tau_a \sigma_c$, brings such difficulty in the determination of emissivity that it will be considered below separately as a Type-7 problem. This occurs as the targets permit repeated cycles of absorption and reflection. The associated Type-7 errors experience geometric growth. It is also clear that, in Eq. (2), the eighth term, $\tau_a \tau_a \sigma_c$, can be paired with normal reflection, σ_{an}, the two being indistinguishable.

The ninth term in Eq. (2), $s_a \tau_a \sigma_c$, generates a Type-5 error as shown in Figure 1B. It accounts for that fraction of the transmitted power which is reflected by the casing, re-enters the absorber, and is then scattered, s_a, into the anechoic chamber. The term resembles a Type-4 error, σ_{td}, involving the effect of diffuse reflection when considering the entire target. However, it is not diffuse reflection, though indistinguishable from such a process. It is properly viewed, as a Type-5 error, as it involves scattering by the absorber following reflection on the casing.

Finally, the tenth term in Eq. (2), $d_a \tau_a \sigma_c$, introduces a Type-6 error. It corresponds to that fraction of the transmitted power which is reflected by the aluminum casing, re-enters the Eccosorb and is then diffracted, d_a, by the edge of the casing into the anechoic chamber (see Figure 1B). The tenth term involves diffraction on the casing from a direction opposite to the incident radiation. It resembles a Type-3 error, Γ_{dc} (previously referred to as Γ_{dt}), in being indistinguishable from it on measurement, but is distinct in its origin. It is real-

ly a "reverse diffraction" since it is produced from radiation which was previously reflected by the metallic casing. It will be properly viewed as a Type-6 error. The distinction is important because, while corrugations can be placed on horns to minimize diffractions on their edges during transmission, they are often not present on the metallic casings of their reference targets [7]. Hence, the diffraction produced as radiation exits the interior of the target is often ignored [7].

If we now represent the seventh through the tenth terms as $\Gamma_{\kappa\sigma}$, $\Gamma_{\tau\sigma}$, $\Gamma_{s\sigma}$, and $\Gamma_{d\sigma}$, Eq. (2) can be re-expressed, with pairing of indistinguishable terms, as follows:

$$\kappa_{t_{\text{eff}}} = (\kappa_t + \Gamma_{\kappa\sigma}) = 1 - (\sigma_{an} + \Gamma_{\tau\sigma}) - (\sigma_{ad} + \Gamma_{s\sigma}) -$$
$$- (\Gamma_{bp} + \Gamma_{dh}) - (\Gamma_{dc} + \Gamma_{d\sigma}) . \quad (4)$$

2.3 Type-7 errors

The most serious problem with microwave target return-loss measurements can be viewed as Type-7 errors which involve the geometry of the targets themselves. This problem exists in all determinations of emissivity from return-loss measurements in the presence of a metal casing. In reality, we are returning to the $\kappa_a \tau_a \sigma_c$, or $\Gamma_{\kappa\sigma}$ term. As previously mentioned, this term does not lead to an error in the return-loss measurement. But, it can cause an enormous error in the determination of emissivity from such measurements. This is a geometric effect, which is best understood by considering targets of varying geometry.

2.3.1 The Planck LFI

Consider, for instance, the target geometry for the ~4 K references on the Planck LFI [7]. These targets are box-like in appearance. They are composed of various layers of Eccosorb, including a small pyramid, enclosed on 5 sides by an aluminum casing (see Figures 8, 10 and 12 in [7]). Given incident radiation from the test horn and neglecting Type-1 through -4 errors, the layer of Eccosorb can initially absorb some of the microwave power. The radiation which is not absorbed is transmitted through the Eccosorb and strikes the aluminum casing. At this point, it ideally experiences normal reflection on the casing and travels back through the absorber. If this radiation is not absorbed following reentry, it travels into space. There, neglecting Type-5 and -6 errors, it can be detected by the horn and registered as return radiation. Note that, now, there are two chances for the incident microwave radiation to be absorbed: first on incidence and then following reflection on the metal casing (term $\kappa_a \tau_a \sigma_c$ above). The situation is not balanced on emission.

Relative to pure emission, the absorber is unable to provide the same performance. For instance, microwaves emitted from the upper surface of the absorber can travel uninterrupted towards the detector. Conversely, radiation emitted through the lower surface of the absorber immediately encounters reflection on striking the metal casing and then re-

enters the material of origin. Once in the absorber, the radiation which had been emitted from the lower surface has a chance of being absorbed before exiting towards the test horn. Furthermore, it is unlikely that the lower surface of such a test target can emit any photons towards the casing, since conduction is also taking place at the interface of the Eccosorb and the aluminum casing (see section 2.4). The effective emissivity, ε_{eff}, of the absorber is reduced by the presence of the metal casing, whereas the effective absorptivity, κ_{eff}, is being increased.

Speaking in quantum mechanical terms, the presence of the metal casing has created a condition where the probability of absorption is no longer equal to the probability of emission. Herein lays the major flaw associated with such approaches. Geometry has produced a condition where return-loss measurements can no longer properly evaluate the effective emissivity of the target. The effective absorbtivity has been enhanced by geometry and the effective emissivity reduced. This is a Type-7 error. Effective radiative equilibrium is being destroyed by geometry and $\varepsilon_{\text{eff}} \neq \kappa_{\text{eff}}$. This occurs precisely because the highly conductive metallic casing ensures that thermodynamic steady state remains. Conduction now compensates for the imbalance created in effective absorptivity and emissivity. In fact, conduction and convection can introduce Type-8 and 9 errors, respectively, as will be discussed in section 2.4.

2.3.2 Pyramidal targets

In order to emphasize the effect of geometry, consider a target where a metal casing is built, composed of a group of small pyramidal structures [10–12]. Such targets are important on geophysical satellites and in radiometry standards laboratories [8, 10–12]. In these targets, each pyramid is about 4 cm in height with a 1×1 cm base [10–12]. A large array of such pyramids, coated with a thin layer of absorber, will form the target. Often, the aluminum casing supports a thin layer of Eccosorb, as seen in the ARIS instrument [8] and other calibration sources [10–12]. In Figure 2A and B, a section of these calibrators is expanded, displaying only the valley created by two adjacent pyramids. Figure 2A treats the situation experienced in measuring absorption from such a target. Conversely, in Figure 2B, emission from a small surface element, at the bottom of the valley, is being considered. In order to simplify the presentation, only absorption and emission towards or away from a single element at the bottom of the valley is considered.

Thus, when radiation is incident on such a structure (see Figure 2A), it has an initial probability of being absorbed when it first enters the Eccosorb, P_1. If the radiation is not absorbed at this interface, it is transmitted to the metal casing where it is immediately reflected. At this point, the radiation re-enters the Eccosorb, where it still has another probability of being absorbed, P_2. Should the photons not be ab-
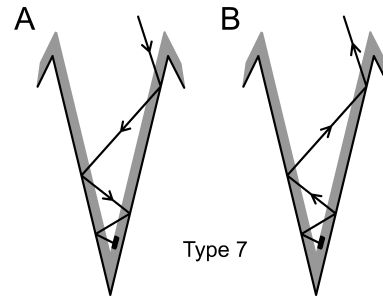

Fig. 2: Schematic representation of geometric, or Type-7 errors, in the assessment of effective emissivity. A) Path of a photon towards an absorptive element at the bottom of the valley. B) Path of a photon emitted by an element at the bottom of the valley. See Table 1 for the effect of geometries on effective emissivity of this element.

sorbed, the radiation travels to the adjacent pyramid. Here, once again, it has a probability of being absorbed, P_3. This scenario continues through many reflections and absorptions. As the photons travel towards the element at the bottom of the valley, a tremendous increase in the probability of being absorbed is generated. This effective absorptivity is made up of the sum of all individual absorption probabilities created from geometry in the presence of the casing. Because of repeated chances of absorption and reflection, the total probability for effective absorptivity, κ_{eff}, is tremendous as shown in Table 1. In fact, this represents geometric growth. For instance, if one permits a total of 8 interactions with the Eccosorp on the way to the small element (9 interactions in total), any photon will have nearly an 87% chance of being absorbed even if the emissivity of the Eccosorb layer (in isolation) was only 0.2. To make matters worse, if that same photon then tries to leave the valley, it must do so while dealing with the probabilities of absorption on exit. Other examples are provided in Table 1. Of course, the effective absorptivity of the target involves the sum of all probabilities for all photons and for all elements. The path through the Eccosorb layers will also be slightly different with each crossing. Nonetheless, it is easy to visualize why these geometric configurations give such outstanding results for effective absorptivity. This is true, even when extremely thin layers of absorber are placed on the surfaces of the metal casing.

Unfortunately, while this situation is outstanding for absorption, it is suboptimal relative to emission. Consequently, a photon produced by a surface element at the bottom of the valley, which is not emitted directly in the direction of the horn, will be subject to repeated chances of being absorbed as it tries to make its way out of this microwave "death valley" (see Table 1). For instance, in considering the reverse path of Figure 2B, we can see that an element with an emissivity of 0.2, will be able to contribute an effective emissivity of only 0.034 after 8 interactions with the Eccosorb (4 changes in direction). Just 4 interactions would more than half the effective emissivity from this element. Once again, the effec-
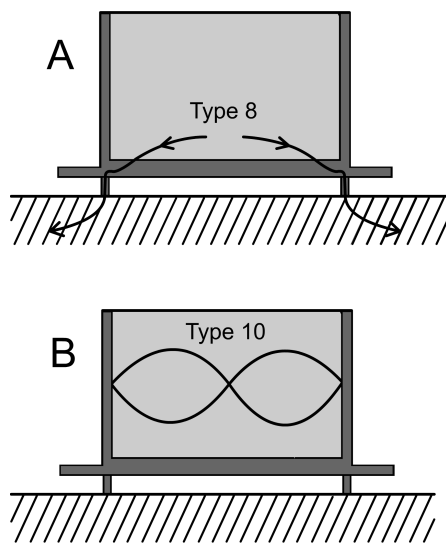
Fig. 3: Schematic representation of A) Type-8, or conductive, errors and B) Type-10, or standing wave errors. These errors can occur when assessing effective emissivity using return-loss measurements.

κ_{eff}	κ	N	ε_{eff}	ε	N
0.865	0.2	8	0.034	0.2	8
0.672	0.2	4	0.082	0.2	4
0.488	0.2	2	0.128	0.2	2
0.2	0.2	0	0.2	0.2	0
0.99	0.4	8	0.0067	0.4	8
0.922	0.4	4	0.0518	0.4	4
0.784	0.4	2	0.144	0.4	2
0.4	0.4	0	0.4	0.4	0
0.99998	0.7	8	0.00005	0.7	8
0.9975	0.7	4	0.00567	0.7	4
0.973	0.7	2	0.063	0.7	2
0.7	0.7	0	0.7	0.7	0

Table 1: Summary of calculated effective absorptivity and emissivity. In this table, κ_{eff} represents the effective absorptivity obtained after N interactions of an incoming photon with the absorber and 1 interaction with the element at the bottom of the valley (see Figure 2). It is assumed that Eccosorb is coating the 4×1×1 cm metallic pyramids [10–12]. The process involves geometric growth as given by $\kappa_{eff} = 1 - (1 - \kappa)^{N+1}$. Similarly, ε_{eff} represents the effective emissivity from a single element obtained after N interactions of an emitted photon with the Eccosorb. If the emitted photon travels directly to the detector, without further interactions with the Eccosorb, then $N = 0$. For effective emissivity, geometric decay is occurring corresponding to $\varepsilon_{eff} = \varepsilon - \varepsilon [1 - (1 - \kappa)^N]$. As a consequece of thermodynamic steady state, it is assumed that the ability of an individual element to absorb or emit radiation remains equal ($\kappa = \varepsilon$). The total effective emissivity of the target constitutes the summation of effective emissivities over all elements, e, and angles (θ and φ): $\varepsilon_{eff_T} = \Sigma\Sigma\Sigma \, \varepsilon_{eff}$.

tive emissivity must include emission over all possible angles. Nonetheless, the situation is unfavorable, as geometry is hindering free emission from most elements.

Moreover, the situation is greatly accentuated if each element of the Eccosorb has a real emissivity of 0.7. In this case, after only 4 interactions with the Eccosorb (2 changes in direction), a photon leaving the bottom of the valley would contribute an effective emissivity of only 0.006. As such, superior absorptive characteristics of the surface absorber lead to inferior performance on effective emission. Furthermore, even a photon emitted near the tips of the pyramid has a chance of doing so in the direction of the valley, not the detector. Such a photon would have almost no chance of escaping the valley. This demonstrates the profoundness of Type-7 errors and the impact of geometry on calibration targets.

It is clear that the probability of absorption or the effective absorptivity, in this geometry, far surpasses the effective emissivity and all return-loss measurements involving such configurations improperly overestimate emission. In fact, rather than building a calibration target which ensures good emission, scientists unknowingly accomplished exactly the opposite. For instance, using infrared imaging, thermal variations in the targets are revealed, wherein the pyramidal tips display a reduced temperature (see Figure 5 in [10]). Such temperature distributions within calibration targets point to the presence of conductive and radiative imbalances which prove that the targets are not black (see section 2.4.1). Figure 5 in [10] constitutes a direct manifestation of Type-7 errors. Relative to emission, it would have been better to provide a very thick surface of Eccosorb. Unfortunately, return-loss measurement would indicate considerable diffuse reflection from such a surface. This had been circumvented by using valleys.

2.4 Type-8, -9 errors

Type-8 and -9 errors can occur when heat flows out of the target through either conductive or convective paths, respectively. To ensure that radiative heat transfer dominates the equilibrium thermodynamics of the target, it is important to minimize all contacts.

A conductive path out of the reference target created with metallic fixtures can set up a Type-8 error as shown in Figure 3A. In this case, it is possible to produce an imbalance between thermal absorption and emission which immediately renders return-loss measurements invalid.

It is evident that a target bombarded with incident microwave radiation on absorption can dissipate such energy through conduction out of the target. It does not need to resort to emission. In this situation, the effective absorptivity of the target will not be equal to its effective emissivity ($\varepsilon_{eff} \neq \kappa_{eff}$), even though thermodynamic steady state is being maintained. This also explains why geometry can produce imbalances in effective emissivity and absorptivity while still maintaining a fixed target temperature.

In theory, a Type-9 error could also be produced, with the same consequences, if convective paths out of the target are

present. Such effects are unlikely to be significant in most scenarios as convective heat transfer is usually ineffective relative to conductive mechanisms.

Consequently, the presence of conduction and convection can introduce two new error terms, Γ_{cond} and Γ_{conv}, such that Eq. (4) now becomes:

$$\kappa_{t_{\text{eff}}} = (\kappa_t + \Gamma_{\kappa\sigma}) = 1 - (\sigma_{an} + \Gamma_{\tau\sigma}) - (\sigma_{ad} + \Gamma_{s\sigma}) -$$
$$- (\Gamma_{bp} + \Gamma_{dh}) - (\Gamma_{dc} + \Gamma_{d\sigma}) - \Gamma_{cond} - \Gamma_{conv}. \quad (5)$$

Conductive and convective errors in target calibration are often not properly addressed and the use of conduction to "cool the target" unwisely advocated [7]. Such approaches highlight elementary errors relative to the understanding of heat transfer. For instance, it is true that conductive paths can be used to heat a target to steady state with all heat being dissipated through radiation. In fact, this was the approach first used to make radiant cavities isothermal [24] in the days which led to Planck's formulation of the blackbody relationship [2, 3]. In this case, conductive paths bring heat into the device which is then forced to escape through radiation. It is quite another matter to permit conductive or convective paths to bring heat out of a target. In the former case, heat leaves the target exclusively through radiation. In the later, it can leave either through radiation or conduction. Accordingly, there is no reason to expect that brightness temperatures in the second setting will be correct.

2.4.1 Max Planck and heat radiation

Relative to this question, Max Planck insists that blackbodies be isolated from the surrounding system. He writes: "*A system of bodies of arbitrary nature, shape, and position which is at rest and is surrounded by a rigid cover impermeable to heat will, no matter what its initial state may be, pass in the course of time into a permanent state, in which the temperature of all bodies of the system is the same. This is the state of thermodynamic equilibrium, in which the entropy of the system has the maximum value compatible with the total energy of the system as fixed by the initial conditions. This state being reached, no further increase in entropy is possible*" [3]. In this treatment, Planck is really making a statement of Prévost's theory of exchanges [25, 26]. However, he is moving beyond Prévost, because he is considering the entropy of the radiation itself. For Planck, the normal spectrum is obtained when the entropy of radiation is maximized [3]. In any case, he continues: "*We shall begin with the simplest case, that of a single medium extending very far in all directions of space, and like all systems we shall here consider, being surrounded by a rigid cover impermeable to heat*" [3]. Finally, Planck makes the point relative to conduction: "*Now the condition of thermodynamic equilibrium requires that the temperature shall be everywhere the same and shall not vary with time. Therefore in any arbitrary time just as much ra-*diant heat must be absorbed as is emitted in each volume-element of the medium. For the heat of the body depends only on the heat radiation, since on account of the uniformity of temperature, no conduction of heat takes place*" [3]. Remember, in this case, that Planck is dealing with a closed system. As such, once thermal equilibrium exists in such a system, there can be no net conduction.

Nonetheless, in open systems, an object can assume a fixed temperature, even if net conduction takes place. Such a situation can be devastating to the production of thermal photons as seen in section 2.4.2.

2.4.2 An example from the remote sensing of soil moisture

Soil moisture can be evaluated through emission profiles in the microwave region [27]. It is well known that the brightness temperature of soil drops dramatically with moisture content [27]. Given the presence of water, the soil can dissipate its heat through conduction, directly into the water, or through convection, as the liquid evaporates. In response, brightness temperatures drop [27]. When soil moisture is removed, brightness temperatures recover, for the simple reason that thermal emission now becomes the primary means of dissipating heat. Placing a body in direct contact with conductive or convective paths, allows heat to escape using non-radiative means, resulting in the lowering of brightness temperatures. In such a scenario, the brightness temperature recorded will be unrelated to the actual temperature of the object of interest. This is precisely what has been done in the case of the LFI reference targets on the Planck satellite [7, 28].

2.5 Type-10 errors

In addition to all of the issues discussed so far, a Type-10 error can exist when standing waves are able to form inside the metal casing, enclosing the absorber (see Figure 3B). Thus, since the casing is made of metal, often possessing a backing along with small walls [7], it introduces the possibility of forming a pseudo-cavity in front of the horn wherein standing waves can build [4]. This leads to a Type-10 error. Such waves would trap energy into the target, making it unavailable to return-loss measurements. Nonetheless, absorption has not occurred. Standing waves simply confine the microwaves [4] and the return-loss measurements suggest an emissivity which is superior to that actually present.

As a result, a complete expression for the determination of absorptivity is as follows:

$$\kappa_{t_{\text{eff}}} = (\kappa_t + \Gamma_{\kappa\sigma}) = 1 - (\sigma_{an} + \Gamma_{\tau\sigma}) - (\sigma_{ad} + \Gamma_{s\sigma}) -$$
$$- (\Gamma_{bp} + \Gamma_{dh}) - (\Gamma_{dc} + \Gamma_{d\sigma}) - \Gamma_{cond} - \Gamma_{conv} - \Gamma_{sw}, \quad (6)$$

where Γ_{sw} accounts for the presence of standing waves. Once again, this term is important in addressing the reference targets on the Planck satellite [28].

3 Conclusions

Much can be gained by carefully considering all thermal components in a heat transfer problem. A complete analysis of error leads to the realization that progress must be made in the fabrication and testing of microwave reference loads and targets. At the same time, these considerations also impact the design of test facilities and anechoic chambers. Ideally, by lining room surfaces with temperature controlled metallic pyramids covered with Eccosorb, it should be possible to simultaneously create tremendous effective absorptivity by the walls and bring their effective emissivity down to very low levels. Such conditions would be ideal in many test scenarios involving anechoic chambers.

At the same time, the measurement of emissivity from microwave targets is a complex problem, wherein up to 10 or more, error types can be identified. Most of these errors are familiar to the geosciences and astrophysics communities. Some may have escaped analysis. Often though, calibration errors have been inappropriately dismissed as insignificant [7]. This is true for Type-10 errors, as the presence of standing waves in the metal casing is almost always ignored [7]. Nonetheless, a greater concern rests in the Type-7 errors which alter the effective radiative balance of the target due to geometrical arguments. Such errors can also be present in calibration blackbodies for use in the infrared [18,19]. Targets are not enclosures [4] and are never blackbodies. Hence, they become subject to geometrical considerations. In addition, Type-8 errors can easily occur raising the possibility that conduction itself, by allowing heat to flow out of the target, is creating an imbalance between effective target emission and absorption. If heat can be funneled out of a target through conduction, its emissivity will fall. This can constitute an important limitation in building calibration targets.

As a result, though attempts have been made to quantify error sources in microwave calibration targets [13–15], it appears that many of the devices used as emissivity references on satellites and in the laboratory (e.g. [4–15] are inaccurate. They are simply unable to provide the emissivity believed to exist using return-loss measurements. This is a significant scientific oversight which affects the monitoring of global climate change (e.g. [8]) and the microwave background [5, 7]. Perhaps it is for this reason that geoscientists are now turning to Earth surfaces as potential calibration sources [29]. Nonetheless, this solution is not available to satellites such as Planck [7, 28] which must rely on their internal reference targets. The proper functioning of spacecraft internal reference targets can have the most profound consequences on scientific advancement, as will be discussed in the accompanying work [28].

Acknowledgements

Dedication

This work is dedicated to Barbara Anne Helgeson.

References

1. Kirchhoff G. Über das Verhältnis zwischen dem Emissionsvermogen und dem Absorptionsvermögen der Körper für Wärme und Licht. *Poggendorfs Annalen der Physik und Chemie*, 1860, v. 109, 275–301 (English translation by F. Guthrie: Kirchhoff G. On the relation between the radiating and the absorbing powers of different bodies for light and heat. *Phil. Mag.*, 1860, ser. 4, v. 20, 1–21).

2. Planck M. Über das Gesetz der Energieverteilung im Normalspektrum. *Annalen der Physik*, 1901, v. 4, 553–563 (English translation by ter Haar D.: Planck M. On the theory of the energy distribution law in the normal spectrum. The old quantum theory. Pergamon Press, 1967, 82–90; also Planck's December 14, 1900 lecture "Zur Theorie des Gesetzes der Energieverteilung in Normalspectrum", which stems from this paper, can be found in either German, or English, in: Kangro H. Classic papers in physics: Planck's original papers in quantum physics. Taylor & Francis, London, 1972, 6–14 or 38–45).

3. Planck M. The theory of heat radiation. Philadelphia, PA., P. Blakiston's Son, 1914, 22–23.

4. Robitaille P.M. Kirchhoff's law of thermal emission: 150 Years. *Progr. Phys.*, 2009, v. 4, 3–13.

5. COBE website, http://lambda.gsfc.nasa.gov/product/cobe

6. Robitaille P.M. COBE: A radiological analysis. *Progr. Phys.*, 2009, v. 4, 17–42.

7. Valenziano L., Cuttaia F., De Rosa A., Terenzi L., Brighenti A., Cazzola G.P., Garbesi A., Mariotti S., Orsi G., Pagan L., Cavaliere F., Biggi M., Lapini R., Panagin E., Battaglia P., Butler R.C., Bersanelli M., D'Arcangelo O., Levin S., Mandolesi N., Mennella A., Morgante G., Morigi G., Sandri M., Simonetto A., Tomasi M., Villa F., Frailis M., Galeotta S., Gregorio A., Leonardi R., Lowe S.R., Maris M., Meinhold P., Mendes L., Stringhetti L., Zonca A. and Zacchei A. Planck-LFI: design and performance of the 4 Kelvin Reference Load Unit. *JINST*, 2009, v. 4, T12006.

8. Lambrigtsen B.H. Calibration of the AIRS microwave instruments. *IEEE Trans. Geosc. Rem. Sens.*, 2003, v. 41, 369–378.

9. Cox A.E. and Janezic M.D. Preliminary studies of electromagnetic properties of microwave absorbing materials used in calibration targets. *IGARSS*, 2006, 3467–3469.

10. Cox A.E., O'Connell J.J., and Rice J.P. Initial results from the infrared calibration and infrared imaging of a microwave calibration target. *IGARSS*, 2006, 3463–3465.

11. Randa J., Cox A.E, Francis M., Guerrieri J. and MacReynolds K. Standard radiometers and targets for microwave remote sensing. *IGARSS*, 2004, v. 1, 698.

12. Feng N. and Wei W. The optimization design for microwave wide band blackbody calibration targets. *International Conference on Microwave and Millimeter Wave Technology* (ICMMT), 2008, v. 4, 1695–1698.

13. Randa J., Walker D.K., Cox A.E., and Billinger R.L. Errors resulting from the reflectivity of calibration targets. *IEEE Trans. Geosc. Rem. Sens.*, 2005, v. 43, 50–58.

14. Li Z., Peng Y., Miao J., Wang Z. Evaluation of disturbance in the antenna calibration of the microwave radiometer. *International Conference on Microwave and Millimeter Wave Technology* (ICMMT), 2008, v. 4, 810–813.

15. Cheng C.Y., Li F., Yang Y.J. and Chen Y.M. Emissivity measurement study on wide aperture microwave radiometer. *International Conference on Microwave and Millimeter Wave Technology* (ICMMT), 2008, v. 4, 914–917.

16. Dietlein C., Popović Z., and Grossman E.N., Aqueous blackbody calibration source for millimeter-wave/terahertz metrology. *Appl. Opt.*, 2008, v. 47, 5604–5615.

17. Robitaille P.M. Blackbody radiation and the carbon particle. *Prog. Phys.*, 2008, v. 1, 36–55.

18. Fowler J.B. A third generation water bath based blackbody source. *J. Res. Nat. Inst. Stand. Technol.*, 1995, v. 100, 591–599.

19. Fowler J.B. An oil-bath-based 293 K to 473 K blackbody source. *J. Res. Natl. Inst. Stand. Technol.*, 1996, v. 101, 629–637.

20. Murphy A.V., Tsai B.K., Saunders R.D. Transfer calibration validation tests on a heat flux sensor in the 51 mm high temperature blackbody. *J. Res. Nat. Inst. Stand. Technol.*, 2001, v. 106, 823–831.

21. Emerson and Cuming Microwave Products. Technical Reference: ECCOSORB CR Two-Part Castable Load Absorber Series. http://www.eccosorb.com/file/958/cr.pdf

22. Stewart B. An account of some experiments on radiant heat, involving an extension of Prévost's theory of exchanges. *Trans. Royal Soc. Edinburgh*, 1858, v. 2(1), 1–20 (also found in Harper's Scientific Memoirs, edited by J. S. Ames: *The laws of radiation and absorption: memoirs of Prévost, Stewart, Kirchhoff, and Kirchhoff and Bunsen*, translated and edited by D. B. Brace, American Book Company, New York, 1901, 21–50).

23. Robitaille P.M. A critical analysis of universality and Kirchhoff's law: a return to Stewart's law of thermal emission. *Prog. in Phys.*, 2008, v. 3, 30–35; arXiv: 0805.1625.

24. Hoffmann D. On the experimental context of Planck's foundation of quantum theory. *Centaurus*, 2001, v. 43(3–4), 240–259.

25. Prévost P. Mémoire sur l'équilibre du feu. Journal de Physique, 1791, v. 38, 314–322 (translated in Harper's Scientific Memoirs (J. S. Ames, Ed.) — *The laws of radiation and absorption: memoirs of Prévost, Stewart, Kirchhoff, and Kirchhoff and Bunsen*, translated and edited by D. B. Brace, American Book Company, New York, 1901, 1–13).

26. Prévost P. Du calorique rayonnant. J. J. Paschoud, Geneva & Paris, 1809 (Sections are translated in Harper's Scientific Memoirs (J. S. Ames, Ed.) — *The laws of radiation and absorption: memoirs of Prévost, Stewart, Kirchhoff, and Kirchhoff and Bunsen*, translated and edited by D. B. Brace, American Book Company, New York, 1901, 15–20).

27. Ulaby F.T., Moore R.K., Fung A.K. Microwave remote sensing active and passive — Volume 2: Radar remote sensing and surface scattering and emission theory. London, Addison-Wesley Publishing Company, 1982, p.884–887.

28. Robitaille P.M. The Planck Satellite LFI and the microwave background: Importance of the 4 K references targets. *Prog. Phys.*, 2010, v. 2, 11–18.

29. Rüdiger C., Walker J.P., Allahmoradi M., Barrett D., Costelloe J., Gurney R., Hacker J., Kerr Y.H., Kim E., Le Marshall J., Lieff W., Marks A., Peisch S., Ryu D., and Ye N. Identification of spaceborne microwave radiometer calibration sites for satellite missions. *Proc. Intern. Congr. Modelling and Simulation* (MODSIM), Cairns, Australia, 2009, 3740–3746.

—————————————